



Study of the Behavior of Beam-to-Column Moment Connections with Tapered Beams

Yousef Hosseinzadeh¹ · Alireza Alimohammadi¹

Received: 16 March 2019 / Accepted: 14 March 2020 / Published online: 23 April 2020
© Shiraz University 2020

Abstract

Steel moment-resisting frames are used as a kind of ductile system to resist earthquake lateral forces. The behavior of rigid beam-to-column connections has a major effect on the behavior of steel moment-resisting frames. In order to provide the required rotational capacity and ductility of connections, some prequalified connections have been proposed in design codes such as the Iranian Building Code (Part 10). In some of the common practices in Iran, a special connection known as tree-column connection is used in which the increasing of the beam section from plastic hinge location to the column's face is provided by a tapered beam section. This connection is not a prequalified connection, and hence, its behavior has not been investigated comprehensively. In this paper, a parametric study was performed using finite element analysis to determine the most influencing geometrical parameters on the behavior of tapered part in such connections (e.g., height and length of the tapered beam). Furthermore, a tapered moment connection (TMC) specimen was tested experimentally to clarify its cyclic behavior. The results obtained provided the use of vertical stiffeners to indicate satisfactory connection performance (TMC) at nonprismatic lengths that extend from 0.8 to 1.2 maximum beam height

Keywords Tapered beam · Ductility · Cyclic testing · Clamped connections · Finite element analysis

1 Introduction

The steel moment-resisting frames (SMRFs) are widely used in a variety of structures. Ductility and the high capacity of the energy depreciation are the key features of these kinds of structures. The beam-to-column connections, as the main part of these frames, resist the lateral forces. The application of SMRF was common from 1964 to 1994. The Northridge and Kobe earthquakes raised serious questions about the reliability of these frames (as shown in Figs. 1, 2). In order to determine the causes of damages in connections during Northridge and Kobe earthquakes, many studies were done. Because of these earthquakes, many brittle failures in the welded beam-to-column connections were shown. As a result of tension concentration in access holes, initial cracks occurred because of applying the support plate below

the flange of the beam, and welding and base metal defects have been one of the causes of these failures (Mahin 1998; Miller 1998). These brittle failures, restricting the inelastic behavior of moment-resisting connections, decreased the ability of connections in bearing the earthquake loads. After Northridge earthquake, to increase the behavior of moment-resisting connections, many studies were done and are being done. Based on research conducted to correct the connection details, suggestions have been put forward. These suggestions (Chen et al. 1996; Plumier 1997; Engelhardt et al. 1998) include decreasing some parts of the beam sections or strengthening the connection so that these actions could provide seismic performance demand under growing cyclic loads behavior of moment-resisting connections.

The philosophy of connections design, after accruing the aforementioned earthquakes, is based on forming a plastic hinge in an appropriate distance of the beam ends. So providing a safe zone for connection of vulnerable parts, the plastic hinge is moved to the inside of the beam. Furthermore, with this plan, the most important structural member of the buildings, i.e., the columns, remains intact. In this case, the beams will absorb the earthquake energy, and the

✉ Yousef Hosseinzadeh
hosseinzadeh@tabrizu.ac.ir

Alireza Alimohammadi
alimohammadi.alireza@znu.ac.ir

¹ Department of Civil Engineering, Tabriz University, 29 Bahman Blvd, Tabriz, Islamic Republic of Iran

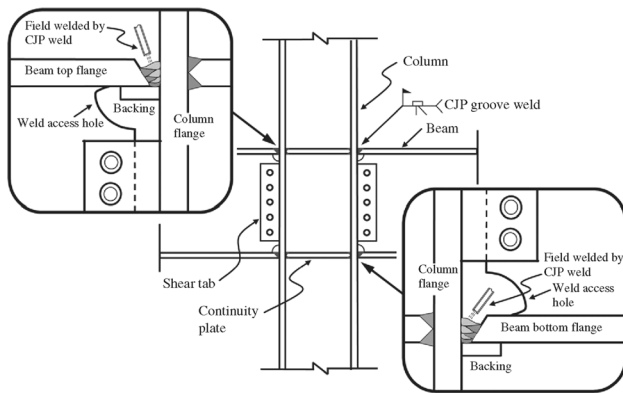


Fig. 1 The pre-Northridge moment connection details

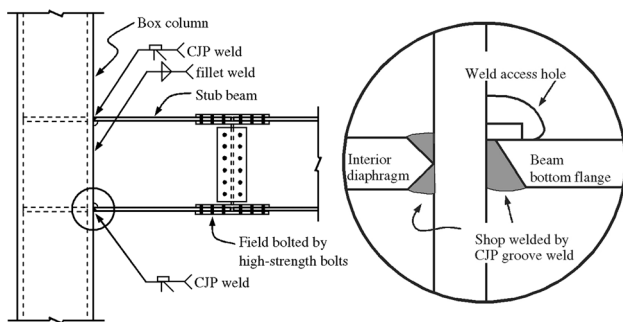


Fig. 2 The pre-Kobe column-tree connection details

remaining intact beams and columns connection would prevent the building from collapsing.

The idea of transferring plastic joints to a distance far from the beam-to-column connection and the expected incremental anchor-to-column connection design has been implemented in Iran by implementation methods referred to as the column-tree method. In the tree-column system, a short element of the beam, about 60–120 cm, is welded to the column in the factory. After installing the tree column in site, the main beam will be screwed to the welded beam. In this method, the factory weld has the appropriate quality and price. Moreover, inspecting the welding process is easy.

Trayana Tankova et al. (2018) studied the buckling behavior of web tapered I-section which is used as the column of industrial buildings. Also, Tankova et al. (2018) carried out some researches on the buckling behavior of these sections as a beam under lateral torsion. Studer et al. (2015) calculated the shear strength of tapered I-shaped steel members in girders, with and without stiffeners.

Demartino et al. (2017) have studied the impact of seismic loss-of-support conditions at frictional beam-to-column connections. Zarsav et al. (2016) studied the effect of stiffener arrangement on hysteretic behavior of link-to-column connections. Zarei et al. (2016) numerically investigated

the seismic performance of rigid skewed beam-to-column connection with reduced beam section. Ghassemieh et al. (2014) have looked into the influence of the axial force on the behavior of end-plate moment connections.

Due to the widespread use of moment connections with a tapered web in Iran, a comprehensive study has not been conducted on their seismic behavior in frames made with box columns. According to AISC385-16 prequalified moment connections for all types of moment frames include reduced beam section (RBS), bolted unstiffened and stiffened extended end plate, bolted flange plate (BFP), welded unreinforced flange-welded web (WUF-W), Kaiser bolted bracket (KBB), ConXtech ConXL, Simpson strong-tie strong frame, double-tee. Therefore, to investigate the seismic behavior and its acceptance or rejection as one of the prequalified connections, they are analyzed in finite element software after examining the basic concepts in the design of tapered webs used in box column construction and determining the parameters affecting the behavior of such connections. Then, by making sure that the parameters in question are implemented, the laboratory model will be developed, and the connection behavior under cyclic loading will be determined following the regulations. Finally, design considerations for these types of connections will be discussed.

2 Design Concept of Tapered Beam Web

2.1 Tapered Beam Web Geometry

Figure 3 schematically illustrates the moment connection of a beam with a tapered web. The purpose of creating a tapered section along the seismic moment slope is to attempt to reach an area with high plastic behavior, which ultimately results in increased moment connection flexibility. The tapered beam consists of a main resistive section and a tapered section. The central resistive part of the beam is attached to the column using full-penetration groove welding, which ultimately results in a significant reduction in seismic moment demand.

The seismic behavior and design of the beam with the tapered web are mainly associated with the flexural capacity of the beam; hence, the moment slope of the flexural capacity and seismic moment demand is shown in Fig. 3. By neglecting the impact of the gravity load, which is often lower than the seismic forces, the flexural strength of the beam required is determined by considering the static equilibrium of the forces with the necessary seismic moment at the plastic joint. For beams with large openings or concentrated loads, the required moment must be calculated based on the conditions in the same beam. According to Fig. 3, when yielding, a range of beams overlaps with flexural capacity and seismic moment demand.

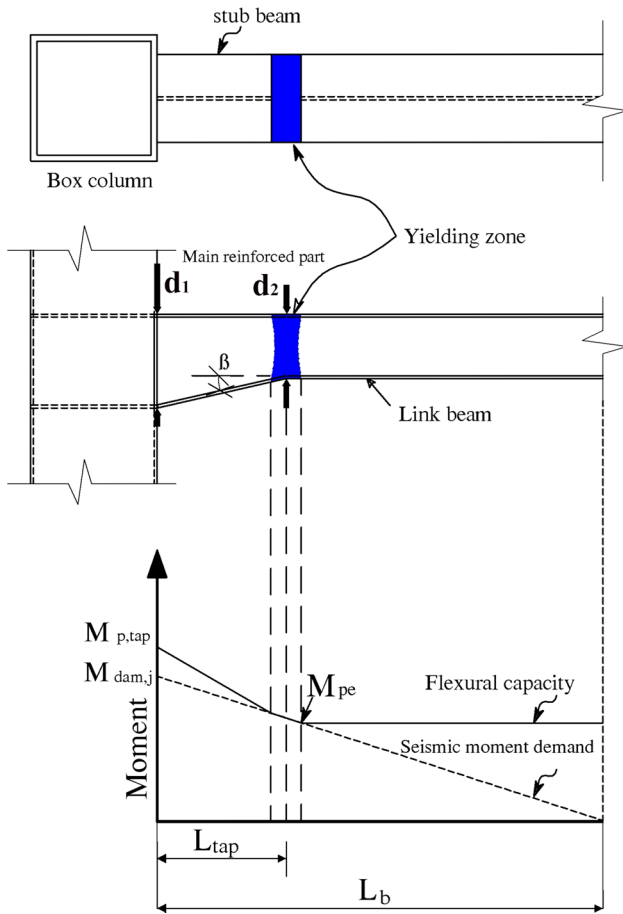


Fig. 3 Properties and moment gradient of a tapered beam web connection

2.2 Design Parameters of Tapered Beam

According to design concepts of the tapered beam web connections, two main parameters related to the connection performance are defined as reinforcement ratio β_j and tapered zone length. To ensure a sufficient rigidity at the beam–column connection, parameter β_j is defined as the ratio of the flexural capacity, M_{pj} , to the seismic moment demand, $M_{dem,j}$ at the beam-to-column connection.

The other main parameter L_{tap} is defined to show the length of beam, the tapered beam, and β reflects the angle between the bottom flange and the line perpendicular to the end of the web in the prismatic beam web.

3 Finite Element Analysis

3.1 Finite Element Modeling

Based on the application of ABAQUS finite element non-linear analysis software, various parameters affecting the

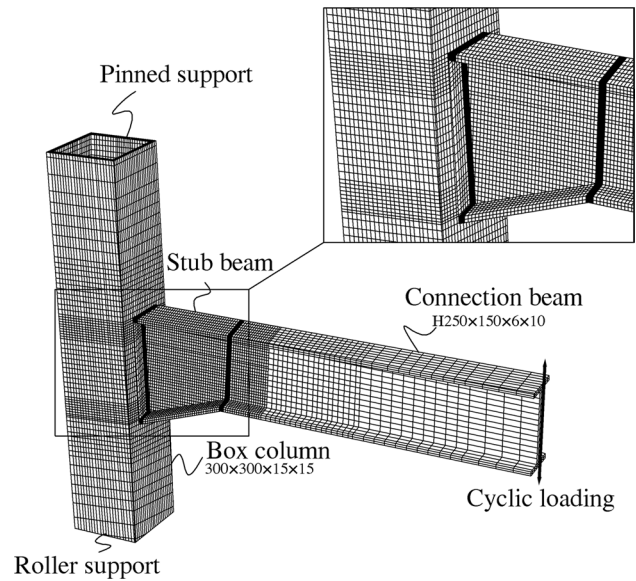


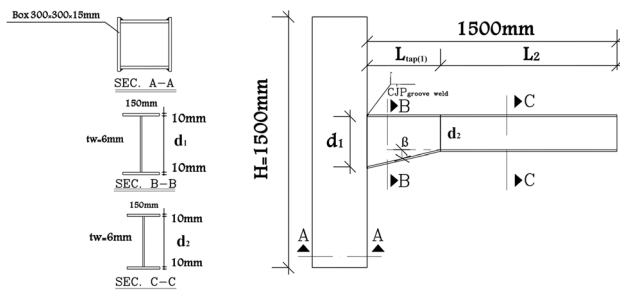
Fig. 4 3D view of the connection FE model

connection of tapered web were modeled and analyzed, and how they influence the connection behavior was investigated. Multiple components of finite element models, including column plates, beam flange, and web with continuity plates, were created using shell-S4R elements. To determine the accuracy of finite element software performance while comparing the results of modeling with standard models, a range of meshing applied in different regions of finite element models was selected by performing sensitivity analysis and its dimensions by defining a specific objective function and performing convergence test (arriving at a difference below 10% in consecutive responses). In Fig. 4, meshing and the boundary conditions of the finite element model are shown in different sections. According to Table 1, 13 models were designed to check the connection details. A conventional connection (e.g., beam-to-column connection) is also provided to compare and evaluate the impact of different parts of the beam with tapered models (UN). Moreover, Table 1 shows the values of the dimensions of different beam sections with the tapered web with a maximum height (d_1) of 265–350 mm and the length of the tapered area ranging from (L_{tap}) 212 to 420 mm. To simplify the stress–strain relationship, the metal structure is modeled based on a two-way isotropic stiffening behavior. Also, the plasticization of the models was determined according to von Mises criteria, and the kinematic hardening behavior was assumed for the cyclic connection performance. The steel used for the initial modeling of the finite element was of A₃₇ type with a yield stress of 240 MPa and ultimate stress of 370 MPa.

In all the models investigated, the ratio of maximum web height to tapered section length is selected equal to 1, 0.8, and 1.2, respectively, to ensure plastic joint formation.

Table 1 Properties used finite element analysis

Number	Finite element models	Reinforcement ratio β_j	Tapered zone length $L_{tap}(\times d_1)$	Tapered angle β (degree)	Length of tapered beam (mm)
1	UN	1.00	–	–	–
2	N265-L0.8	1.06	0.8	4	212
3	N265-L1	1.06	1	3.2	265
4	N265-L1.2	1.06	1.2	2.7	318
5	N285-L0.8	1.16	0.8	8.7	228
6	N285-L1	1.16	1	7	285
7	N285-L1.2	1.16	1.2	5.8	342
8	N300-L0.8	1.24	0.8	11.8	240
9	N300-L1	1.24	1	9.5	300
10	N300-L1.2	1.24	1.2	8	360
11	N350-L0.8	1.5	0.8	19.6	280
12	N350-L1	1.5	1	15.9	350
13	N350-L1.2	1.5	1.2	13.4	420

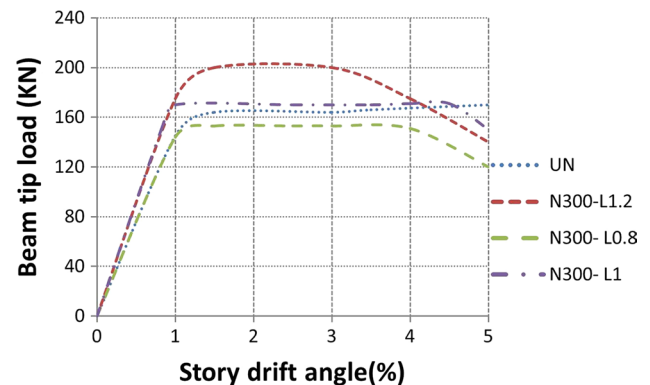
**Fig. 5** General details of connection geometry

General connection details investigated are presented in Fig. 5. Each model is named from two sections as NA-LB, with A and B representing d_1 and d_1-L_{tap} ratio, respectively. It should be noted that these two sections have been reviewed and provided in the initial design of the connections of all the requirements of the by-laws concerning steel sections, especially those which must be observed at the nonprismatic junction to the main beam. Furthermore, according to the objectives of this study, the sections used are of a compact seismic type.

3.2 Discussion of the Results

The graph related to the end forces of the beam to the lateral displacement angle for some particular models is shown in Fig. 6. The relative displacement angle is obtained from dividing the displacement of the end of the beam to the distance between these points to the column center.

As long as the lateral displacement is less than 1%, all of the models have elastic behavior, which is suitable for moment-resisting frames with common ductility. In spite of the increased web height, most of the models have more

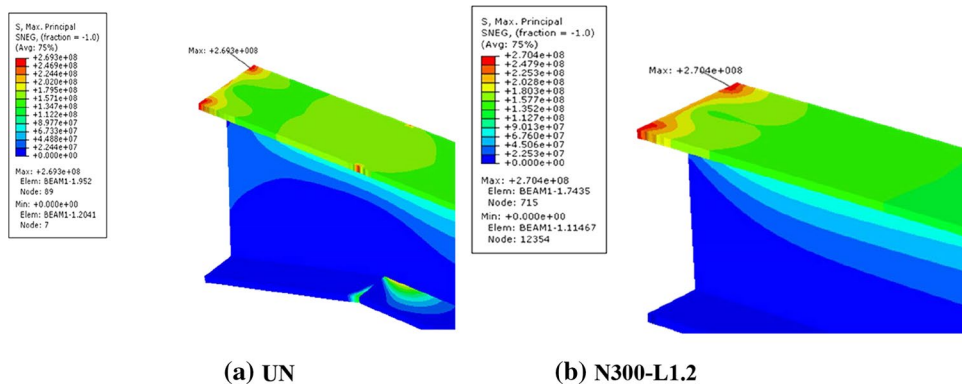
**Fig. 6** Beam tip load versus story drift angle relations for N300 and UN models

elastic stiffness and inelastic strength than model UN. However, this increase in height and length in the tapered section will lead to inverse results after a certain amount.

For instance, the samples 4, 7, 10, 13 experienced a decrease in the strength after relative displacement of 3%, which shows the crippling of web in a zone where the tapered and untapered parts are connected. In this case, the samples 3, 6, 9, 12 show the proper results in the area.

It should be mentioned that because many moment-resisting connections experience premature damages during earthquakes in their plastic range, the lateral drift ratio is considered to be 0.5% to specify the elastic response of the finite element models. In order to evaluate the potential of brittle failure, given that many cracks occurred close to the main maximum tensions, the place of these tensions is specified in the models. Figure 7 shows the principal stress vectors and the stress contour for the N300-L1.2 and UN models at a drift angle of 0.5%.

Fig. 7 Distributions of principal stress vectors and contours at the beam–column interface at 0.5% rad story drift angle



The observations show that the maximum tension of the moment connection happens at the beam flange where the complete penetration groove weld is performed. The maximum value of the main tension (normalized to yield tension of the beam material) at the model UN is obtained equal to 1.127, while this value for the model N300-L1.2 is decreased in 1.122. The maximum tension at both cases occurs in the edges.

From Fig. 8, the study of the tapered moment connections cyclic behavior shows weakness in it. The high deflections are clearly recognized when the relative displacement is more than 2%. Therefore, using these kinds of connections, as they are illustrated in Fig. 8, it is practically impossible for them to be used for special or intermediate moment-resisting frames. Therefore, in order to improve the behavior of these kinds of connections, using horizontal and vertical stiffeners seems appropriate.

After using the different kinds of stiffeners in the vertical and horizontal situations and studying their effect on improving the behavior of these kinds of connections, it is concluded that using two pairs of vertical stiffeners at a distance of $1.5B_f$ (B_f is the width of the beam flange), two pairs of horizontal stiffeners about one-third the height of the cross section yielded good results. The height of each stiffener is equal to the height of the web, and its width is half the width of the beam.

To apply these stiffeners, all of the criteria such as preventing local buckling are considered. In Fig. 9, the different ways of applying the stiffeners, for the vertical and horizontal cases, are shown for the models.

The behavior of connections within inelastic range could be evaluated through the plastic strain. In order to study the local plastic strain demand, the response of the model components is defined by PEEQ index. This statement stands for the equivalent plastic strain, which shows local plastic strain demand. The PEEQ index is driven from the value of the equivalent plastic strain to the yield strain. It is obvious that the higher the PEEQ index, the more the plastic strain demand will be, since the acceptance criterion for the special moment-resisting frames is no decrease in the strength at a drift angle of 4%.

In Fig. 10, PEEQ index is specified in the connection flange weld of the tapered beam in drift angle of 5% for the cases of without stiffener and two couple of horizontal (2stH) and vertical (2stV) stiffeners. As it is recognizable from the figure, for model N300-L1.2, the maximum amount of PEEQ index is happened in weld at the outer edge of the flange of the beam, while PEEQ index in the other models in comparison with the model N300-L1.2 has no considerable decrease. Due to the occurrence of nonelastic web buckling at the junction of the tapered beam to the prismatic part, it was not possible to increase the cross-sectional capacity.

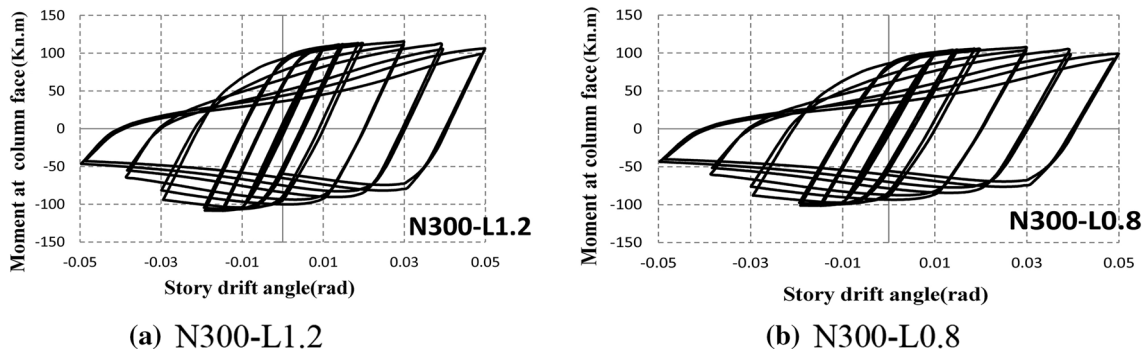


Fig. 8 Moment–rotation relationships for models (a)N300-L1.2, (b) N300-L0.8

However, if stiffeners are used, especially vertical stiffeners, appropriate improvements in this index are observed at the beam-to-column junction as an increase in the cross-sectional capacity.

To consider the process of becoming plastic in the section and forming plastic hinges at the tapered connections, different distributions of equivalent plastic strain are shown in Fig. 11 for the model N300-L1. The increase in the contour of equivalent plastic strain for drift angles 1%, 1.5%, and 5% shows that the maximum equivalent plastic strain does not occur in the penetration groove weld of the flange of the beam, but it forms in an area far from the column face. This area is located in the connection zone of the tapered part to the untapered. By applying stiffeners, especially vertical

stiffeners, the plastic hinge moves a little into the tapered part, increasing loading capacity during cyclic loading.

To compare the models above in Fig. 12, the beam force enveloping curves on the support are plotted against relative displacement. As can be seen in these diagrams, in case of using vertical stiffeners, all samples are equally resistant to a 40-mm displacement at the end of the beam (3% drift). Samples with a taper equal to the maximum height of the beam web are slightly more resistant than other samples. After this percentage, plastic buckling displacement begins in the beam flange and web. Overall, it can be concluded that the effect of the tapered section length on the overall behavior of the sample is negligible if the stiffener is used up to 3% relative displacement.

Fig. 9 Make use of stiffeners

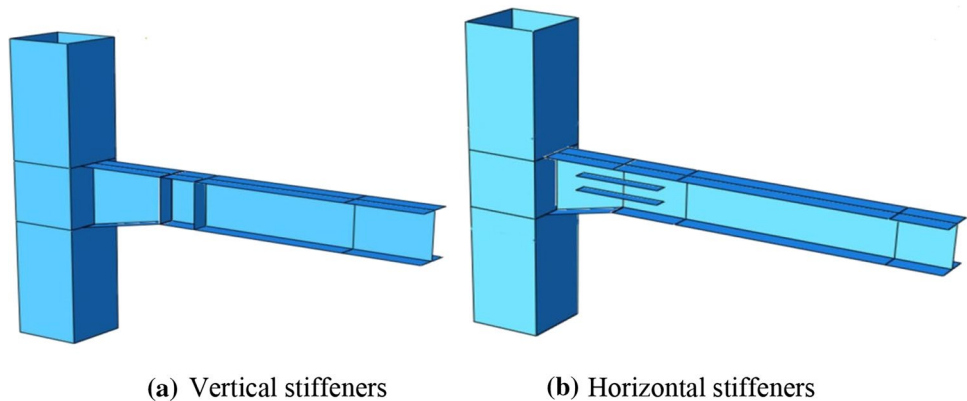


Fig. 10 The PEEQ index diagram at penetration groove weld for drift angle of 5 %

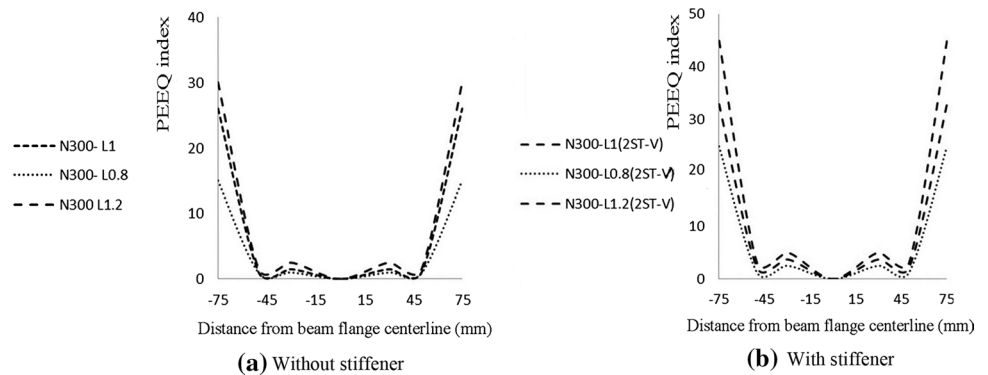
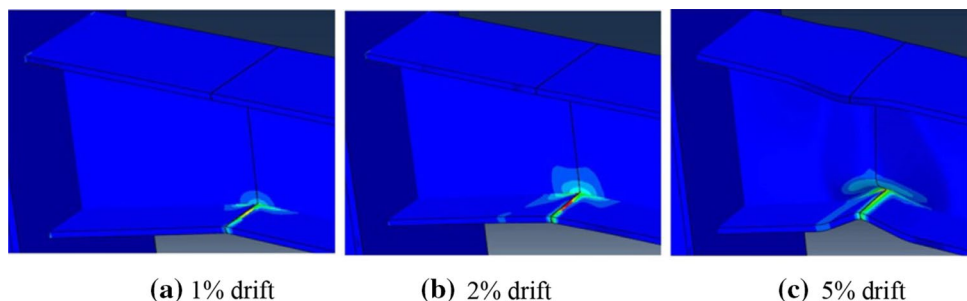


Fig. 11 Plastic equivalent strain contours of N300-L1 at 1, 2, and 5% rad story drift angles



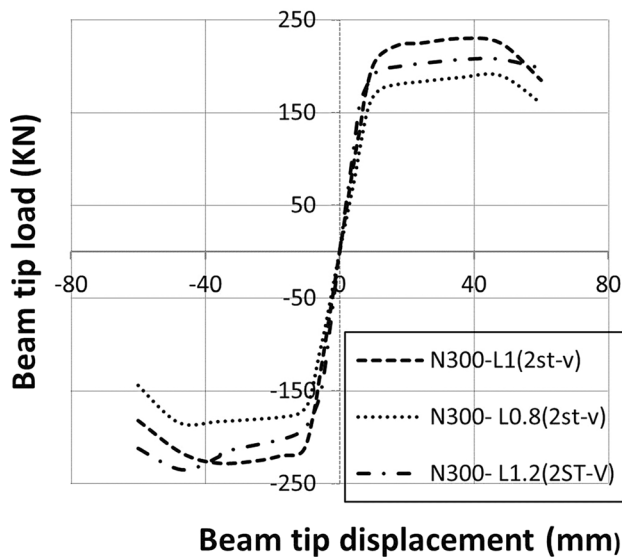


Fig. 12 Envelope curves of beam tip load–displacement relations

Table 2. Material properties

Member	Coupon location	Steel type	Yield strength F_y (Mpa)	Ultimate strength F_u (Mpa)
Beam	Beam flange	A37	295	420
	Beam web	A37	310	425
Column	Column flange	A37	300	438

Table 3. Test specimens

Specimen designation	Reinforcement β_j	Tapered zone length $L_{tap} (\times d_p)$	Connection details
N300-L1.2(2st-v)	1.25	1.2	Column-tree connection, beam web welded

4 Experimental Program

4.1 Test Specimens

The test plan was developed to compare the behavior of column-tree connection with a tapered beam with numerical samples investigated. In this experiment, a real-scale N300-L1.2 (2st-v) sample was fabricated. The mechanical properties of the steel used for the fabrication of this sample are following the specifications provided in Table 2, taking into account the test coupons. The main I-shaped beam with dimensions of $10 \times 150 \times 6 \times 250$ is equal to

the web height, web thickness, flange width, and flange thickness, respectively. Also, the column is made of a box section with dimensions of $15 \times 15 \times 300 \times 300$. In this experiment, the beam is attached to the column using full penetration weld. To prevent any slide and subsequent impact on the connection behavior, the beams are also connected by welding. Table 3 shows the main parameters of the test beam, including length and height. The two main parameters include the length and height of the tapered beam of the test sample, according to Table 3.

4.2 Test Setup and Loading

The schematic diagram of the experimental setup is shown in Fig. 13, in which the sample specifications and support conditions are described. The lateral force is applied by an actuator with a speed of 10 mm per minute in the form of quasi-static and without acceleration toward the end of the beam is applied. The loading protocol is considered based on AISC 385-16 code (AISC 2016) to study the cyclic states. This loading, according to Fig. 14, is started from the drift angle of 0.375–5%. During the test, also in order to fit more into reality, another actuator applies a constant load to the column. The overview of the sample is shown in Fig. 15.

4.3 Discussion of the Test Results

According to the results of FEM, the initial yield point was at the edge of the tapered beam flange. When the angle of rotation becomes more than 3%, there would be relatively high displacements at the column-to-the main beam junction.

For the rotation angle of 4%, the local inelastic buckling is occurred at the bottom flange of the tapered zone.

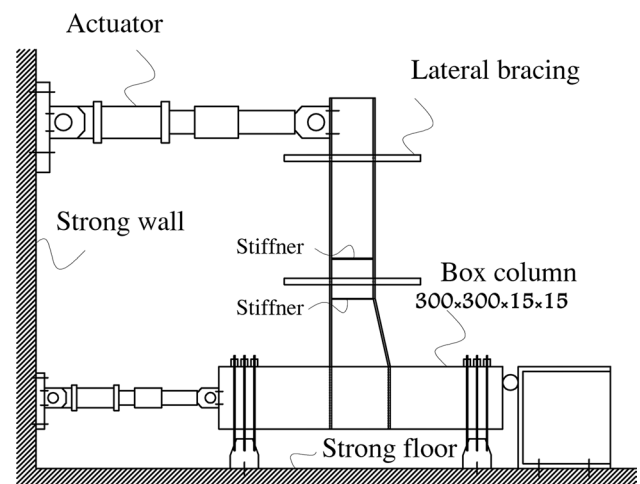


Fig. 13 Schematic diagram of the test setup

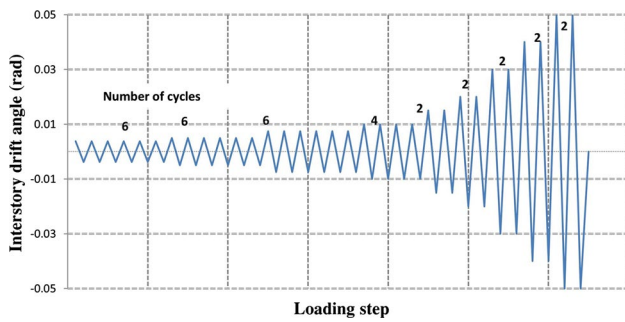


Fig. 14 The loading protocol

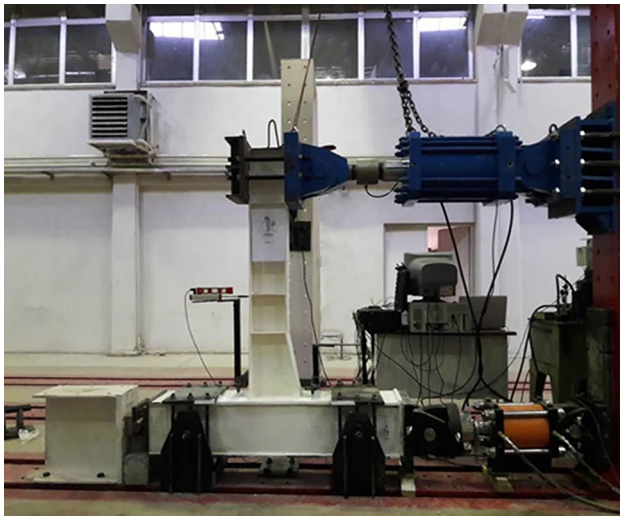
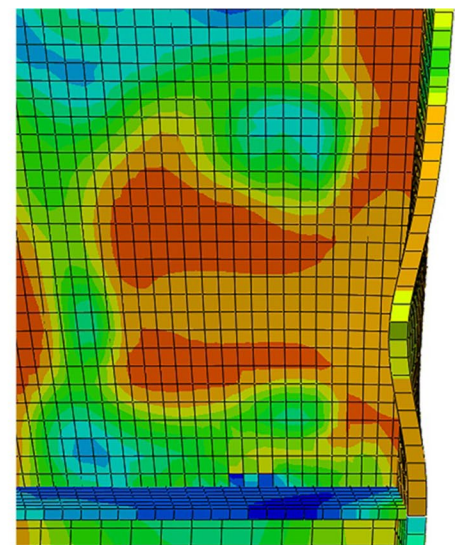


Fig. 15 Test setup

Fig. 16 Comparison of failure mode between FEM and test



(a) N300- L1.2 (2st-v)



(b) Finite element

The yield and the local buckling at the flange for sample N300-L1.2 (2st-v) are shown in Fig. 16. At the rotation angle of 5%, increasing the amount of the buckling at the beam flange, the strength of the connection decreases gradually. For all samples, the plastic hinge appears at a point far from the beam–column connection. It ensures inelastic deformations at the joint at the end of the test. There are no signs of failure and break at the joint of beam and column.

To assess the cyclic behavior of connections, the force–displacement hysteresis loops are generally used for verification. The loading and drift graph are plotted in Fig. 17 for the experimental sample.

For a better comparison, the amount of total plastic rotation is normalized with respect to the plastic moment of the section.

With the use of experimental results, the calculated ultimate moment, and displacement, it is possible to obtain moment–rotation hysteresis loop for experimental sample. This graph is represented in Fig. 18 for N300-L1.2 (2st-v) sample.

This graph also shows an appropriate adaptation with the result of FEM. As plastic rotation can be obtained from total rotation minus elastic rotation, with regard to the elastic behavior of the column and the connection panel during experimentation, the obtained total rotation is the plastic rotation that has been considered in the final result. Since the plastic rotation of the section is obtained from the subtraction of the elastic rotation from the total rotation, and given that the column and the panel zone had elastic behavior during the experiment, the plastic rotation will be obtained directly from the plastic deformation of the beam.

As seen in Fig. 18, the resulting hysteresis loops show a reliable cyclic behavior, and the gradual decrease in the ultimate strength is due to local buckling at the flange of the

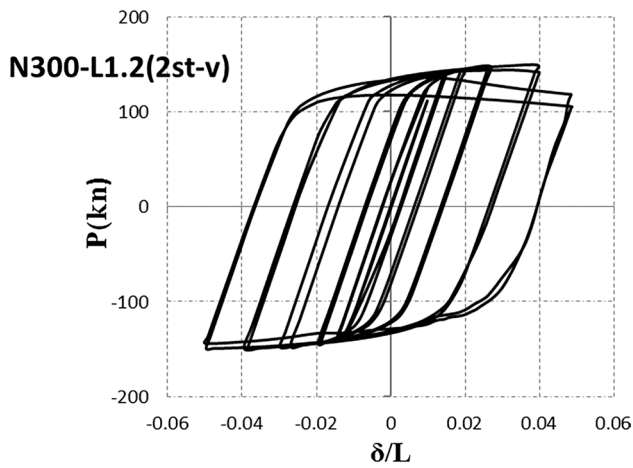


Fig. 17 Hysteretic curves for N300-L 1.2(2st-v) experimental sample

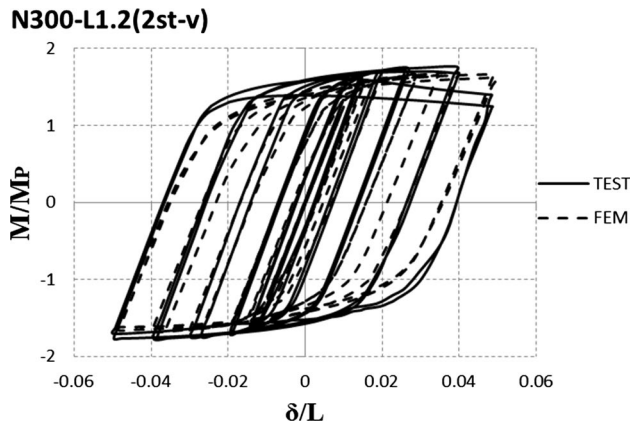


Fig. 18 Comparison of normalized story moment versus drift between FEM and test for N300-L 1.2 (2st-v) experimental sample

tapered beam. Samples can show the reliable cyclic behavior up to angle 5% with the maximum plastic rotation 4–4.9% radian, so that it is possible to accept the obtained results.

5 Design considerations

In order to simplify the design, the thickness of the beam flange and web, and beam depth of the tapered beam web connection are assumed to be the same as the main beam. Based on results, the length of the tapered zone recommended 0.8–1.2 days. The design method could be summarized as follows:

First, the expected plastic moment of the beam, M_{pe} , is calculated by: $M_p = R_y F_y Z_b$ where $R_y F_y$ is the expected yield strength and Z_b is the plastic section modulus for main beam.

Second, the maximum height of the tapered beam web is determined by calculating the design flexural capacity at the beam-to-column joint as follows:

$$M_{p,j} = M_{p,tap} \tag{1}$$

$$M_{p,tap} = \beta_j M_{dem,j}$$

where $M_{dem,j}$ represents the moment demand of the beam at the beam-to-column joint and is calculated as follows:

$$M_{dem,j} = \left(\frac{L_b}{L_b - L_{tap}} \right) M_{pe} \tag{2}$$

According to test results, β_j can be set to 1.15 or greater to prevent failure at the groove weld of the connection. Moreover, the shear demand in the web of the tapered beam web at the beam-to-column joint, $V_{dem,j}$, must be determined to ensure sufficient capacity at this critical section. Design shear for this zone can be calculated as:

$$V_{dem,j} = \left(\frac{M_{dem,j}}{L_b} \right) + V_g \tag{3}$$

where V_g is the shear at the column face due to gravity loads. It is necessary to mention that because of creating a tapered section the flexural capacity of the beam increases at the beam-to-column joint, and the weak beam–strong column criteria should be controlled.

6 Conclusions

A preliminary laboratory study was carried out about the effect of the length of the tapered zone on the behavior of column-tree connections using these connections. According to the results, the cyclic behavior of suggested tapered connections for column-tree MRF shows that the plastic hinge is formed at a zone far from column face, which is located at the intersection of the tapered and nontapered parts. These kinds of connections are typically used in ordinary MRF. However, according to the results, this kind of connection does not have the ability to satisfy requirements about plastic deformations and needed strength related to special MRF. The occurrence of plastic buckling at the beam section and the unbalanced state of the tapered part lead to an intense asymmetry at the cyclic behavior, so that the strength drops dramatically. Therefore, to compensate for these defects, the vertical stiffeners were applied. For all cases, the plastic hinge is formed far from column face. Therefore, it satisfies the requirements of AISC358-16.

Hysteresis loops show the stability and the strength of samples at the cyclic behavior. The drop of resistance, which is occurred in some loops, is because of the occurrence of the local plastic buckling at the web and flange of the beam.

All samples, reinforced with vertical stiffeners, can properly bear the inelastic behavior around the drift angle 5% rad. The maximum plastic rotation has happened at the drift range of 4% to 4.9% rad. According to AISC-2016, a connection is acceptable if the moment at the column face, in the 4% drift angle, is greater than 80% of the plastic moment of the beam. However, to determine other effective factors on the behavior of this connection accurately, more studies on the different dimensions of the beam, the column, and H-shape columns are needed. Due to time and energy constraints, less parameters were studied in this thesis.

References

- AISC358-16(2016) Prequalified Connections for Special and Intermediate Steel Moment Frames for Seismic Applications, Chicago (IL) American Institute of Steel Construction.
- Chen SJ, Yeh CH, Chu JM (1996) Ductile steel beam-to-column connections for seismic resistance. *J Struct Eng* 122(11):1292–1299
- Demartino C, Monti G and Vanzi I (2017) Seismic loss-of-support conditions of frictional beam-to-column connections, *Struct Eng Mech* 61(4).
- Engelhardt MD, Winneberger T, Zekany AJ, Potyraj TJ (1998) Experimental investigation dogbone moment connections. *Eng J* 35:128–139
- Ghassemieh M, Shamim I and Gholampour AA (2014) Influence of the axial force on the behavior of endplate moment connections, *Struct Eng Mech* 41(1).
- Mahin ST (1998) Lessons from damage to steel building during the Northridge earthquake. *Eng Struct* 20(4–6):204–216
- Miller DK (1998) Lessons learned from the Northridge earthquake. *Eng Struct* 20(4–6):249–260
- Tankova T, Pedro Martins J, Simões da Silva L, Simões R, Craveiro HD (2018) Experimental buckling behaviour of web tapered I-section steel columns. *Journal of Constructional Steel Research* 147:293–312
- Tankova T, Pedro Martins J, Simões da Silva L, Marques L (2018) Experimental lateral-torsional buckling behaviour of web tapered I-section steel beams. *Engineering Structures* 168:355–370
- Studer R, Binion C, Davi D (2015) Shear strength of tapered I-shaped steel members. *J Constr Steel Res* 112:167–174
- Plumier A (1997) The dogbone: back to the future. *Eng J* 2:61–67
- Zarei A, Vaghefi M and Fiouz A.R (2016) Numerical investigation seismic performance of rigid skewed beam-to-column connection with reduced beam section, *Struct Eng Mech* 57(3).
- Zarsav S, Zahrai S M and Vatani Oskouei A (2016) Effect of stiffener arrangement on hysteretic behavior of link-to-column connections, *Struct Eng Mech* 57(6).